Journal of Geochemical Exploration 175 (2017) 36–47

Contents lists available at ScienceDirect

Journal of Geochemical Exploration

journal homepage: www.elsevier.com/locate/gexplo

# Modes of occurrences of major and trace elements in coals from Yangquan Mining District, North China

Qiming Zheng [a], Songlin Shi [a], Qinfu Liu [b,*], Zhanjie Xu [b]

[a] School of Resources and Environment Engineering, Henan University of Engineering, Zhengzhou, Henan 451191, China
[b] School of Geological Science and Survey Engineering, China University of Mining and Technology, Beijing 100083, China

ARTICLE INFO

*Article history:*
Received 9 August 2016
Revised 12 November 2016
Accepted 7 December 2016
Available online 12 December 2016

*Keywords:*
Yangquan
Coal bench
Mineral assemblage
Trace element

ABSTRACT

Yangquan Mining District is a major location for anthracite coal production in China. Understanding the modes of occurrences of major and trace elements in Yangquan coal is significant both geochemically and environmentally, although most elements are more depleted than those in Chinese coal. Ten coal bench and two parting samples were collected from No. 15 Coal of Yangquan Mining District. X-ray diffraction analysis was used to determine the proportions of minerals in the Yangquan coal, and X-ray fluorescence and inductively coupled plasma mass spectrometry analyses were used to determine the contents of major element oxides and trace elements, respectively. The mineral assemblages, ash yield, and $(CaO + MgO + Fe_2O_3)/(SiO_2 + Al_2O_3)$ ratio varied significantly in the vertical direction, which is attributed mainly to vertical variation in the depositional environment. The major element oxides and trace elements in the Yangquan coal were divided into four groups according to cluster analysis, which represent organic or inorganic affinity and different modes of occurrences. The coal benches underlying partings exhibited a rare-earth element and yttrium (REY) distribution pattern characterized by heavy (H)-type. This result differs from other coal benches characterized by light (L)-type REY, which is attributed to the leaching of overlying partings.



## 1. Introduction

Coal is composed of organic and inorganic matter containing various major and trace elements that have inorganic or organic affinity (Ren et al., 2006; Dai et al., 2012a; Rajabzadeh et al., 2016; Sutcu and Karayigit, 2015; Ward, 2016). The main carriers of major and trace elements in coal are mineral matter, the assemblages of which can in turn indicate the occurrence modes and origins of these elements. In addition, these mineral assemblages can reveal characteristics of geological process such as depositional environment, degree of diagenesis, maturation, epigenesist, and the influence of groundwater (Ren et al., 2006; Ward, 2002; Dai et al., 2012b; Jiang et al., 2015). Dai et al. (2006) described vertical variations in $Al(OH)_3$ minerals and enriched Ga in the No. 6 Coal of Junger Coalfield that resulted from changes in terrigenous origin. Shi et al. (2014), Wu et al. (2013), and Wang et al. (2011b) also reported significant enrichment of Al and Ga in the same coal. Zheng et al. (2016) suggested that compared to fresh water, seawater is more favorable for the formation of ammonian illite during deposition. The ratios of $(CaO + MgO + Fe_2O_3)/(SiO_2 + Al_2O_3)$ and U/Th and B content in coal can be used as indicators of depositional environments (Ren et al., 2006; Goodarzi and Swaine, 1994a, 1994b). Carbonate minerals in coal dominated by calcite and dolomite are generally epigenetic rather than authigenic or detrital owing to the acidic environment during peat accumulation (Belkin et al., 2010; Bouška et al., 2000; Dai et al., 2012a). The parameters associated with rare earth elements and yttrium (REY) in coal, such as the REY distribution pattern, δEu and $La_N/Lu_N$, can be used as indicators of the sediment-source region, depositional environment, and post-depositional conditions (Seredin, 1996; Ren et al., 2006; Eskenazy, 1987; Hower et al., 1999; Dai et al., 2010). In addition, trace elements in coal have significant effects on the environment (Tozsin, 2014; Sia and Abdullah, 2011; Liu et al., 2015; Ali et al., 2015; Zheng et al., 2008; Sahoo et al., 2014). Some elements, particularly toxic trace elements such as Zn, Cu, Cd, and Ni, are generally not enriched in coal but are significantly enriched in coal-related atmospheric particulate matter; these toxic trace elements are derived mainly from coal mining, combustion, and utilization (Lewińska-Preis et al., 2009; Song et al., 2015a; Lv et al., 2006). Coal mining, combustion, and utilization have contributed significantly to the severe atmospheric particulate pollution in North China in recent periods (Song et al., 2014, 2015a, 2015b). Therefore, it is of geochemical and environmental significance to understand the contents, affinity, and modes of occurrences of major and trace elements in coal.

* Corresponding author.
*E-mail addresses:* zqm6502644@163.com (Q. Zheng), lqf@cumtb.edu.cn (Q. Liu).

http://dx.doi.org/10.1016/j.gexplo.2016.12.008
0375-6742/

The coal from the Qinshui Coalfield, North China, is dominated by anthracite coal and has relatively low coal ash yield (Qin et al., 1999). Most elements in this coal are significantly depleted compared with other coal in China and abroad owing mainly to the low ash yield (Tang et al., 2013; Dai et al., 2012b). However, some toxic trace elements derived from coal mining, combustion, and utilization dominated by chalcophile elements are significantly enriched in atmospheric particulate matter (Song et al., 2015a). This paper presents the mineral assemblages, content of major element oxides, and trace elements in the coals of the Qinshui Coalfield. The objectives of this study are to investigate the variation in depositional environments and mineral assemblages and to examine the inorganic or organic affinity and modes of occurrence of various major element oxides and trace elements in this coal.

## 2. Geological setting

The Yangquan Mining District is located in the northern region of the Qinshui Coalfield and covers an area of 1400 km$^2$ (Fig. 1; Jiao and Wang, 1999). This mining district is a location of major anthracite coal production in China and has a proven coal reserve of 141.8 Gt (2013; Zhu, 2013). The Yangquan Mining District has an annual production capacity exceeding 100 Mt and includes several large-scale coal mines such as First Coal Mine, Second Coal Mine, Fifth Coal Mine, Xinjing Coal Mine, Sijiazhuang Coal Mine, and others (Xu and Sun, 2009; Zhu, 2013). The coal-bearing strata in the Yangquan Mining District are situated in the Carboniferous Taiyuan and Permian Shanxi formations, with average thicknesses of 120 m and 46 m, respectively (Fig. 2). The Carboniferous Taiyuan Formation conformably overlies the Carboniferous Benxi Formation and is composed mainly of white feldspar–quartz sandstone, dark gray limestone, dark gray siltstone, sandy mudstone, and coal. The minable coal seam in this formation is dominated by No. 15 Coal, followed by Nos. 8, 9, 12 and 13 coals. The Permian Shanxi Formation conformably overlies the Taiyuan Formation and is composed mainly of gray–white feldspar–quartz sandstone, dark gray siltstone, sandy mudstone, and coal, and the minable coal seam in this formation is dominated by No. 3 Coal, followed by Nos. 2 and 6 coals. The No. 15 Coal is the sampling coal seam, which varies in thickness from 5.0 m to 8.7 m (Ge et al., 1985; Jiao and Wang, 1999). The strata overlying the Shanxi Formation are included the non-coal-bearing Permian Lower Shihezi Formation (Wang et al., 1998; Jiao and Wang, 1999). The No. 15 Coal is dominated by anthracite coal and has a total sulfur content varying from 1.7% to 3.5% with an average of 2.3% (Fu and Wu, 2012). According to Chinese Standard GB/T 15224.2-2004 (2004), the No. 15 Coal is a middle- to high-sulfur coal. The peat for No. 15 Coal accumulated prior to large-scale transgression in a brackish water swamp of a coastal plain and was influenced by seawater during and after the accumulation; this resulted in the relatively high total sulfur content (Jiao and Wang, 1999). The No. 15 Coal in the Yangquan Mining District contains two relatively continuous intra-seam mudstone partings, Bacunshi and Lvshi, with thicknesses of 0.10 m and 0.20 m, respectively.

## 3. Samples and methods

### 3.1. Sample collection

The sampling coal mine in the present study is First Coal Mine, which is located in the northern Yangquan Mining District. The No. 15 Coal in First Coal Mine has an average thickness of 5.3 m. From this coal, 10 coal bench samples were continuously collected from roof to floor following the procedure described in Chinese Standard Method GB/T 482-2008 (2008), and each coal bench was cut over an area with 10-cm wide and 10-cm deep with a thickness of 0.5 m; two continuous intra-seam partings were also collected. The numbers of coal samples from the roof and floor are YQ1-15-C1 to YQ1-15-C10, and the numbers of the two intra-seam partings are B-P and L-P (Fig. 3). Once collected, all of the samples were immediately stored in plastic bags to avoid contamination and deliquescence.

### 3.2. Ash yield and volatile matter

The ash yield on a dry basis and volatile matter on a dry and ash-free basis for the coal samples in the present study were determined according to American Society for Testing and Materials (ASTM) Standards D3174-04 (2005) and D3175-02 (2005).

### 3.3. X-ray diffraction (XRD) analysis

The coal and parting samples were crushed and ground to <200 μm for the following analysis. The minerals in the coal and parting samples were identified by X-ray diffraction (XRD) analysis. The XRD pattern of each sample was examined by using Quan software, developed by Lin (1990), to quantitatively calculate the proportion of each mineral phase identified by XRD analysis according to the methods proposed by Chung (1974a, 1974b, 1975) and outlined in Chinese Petroleum and Gas Industry Standard Method SY/T 5163-

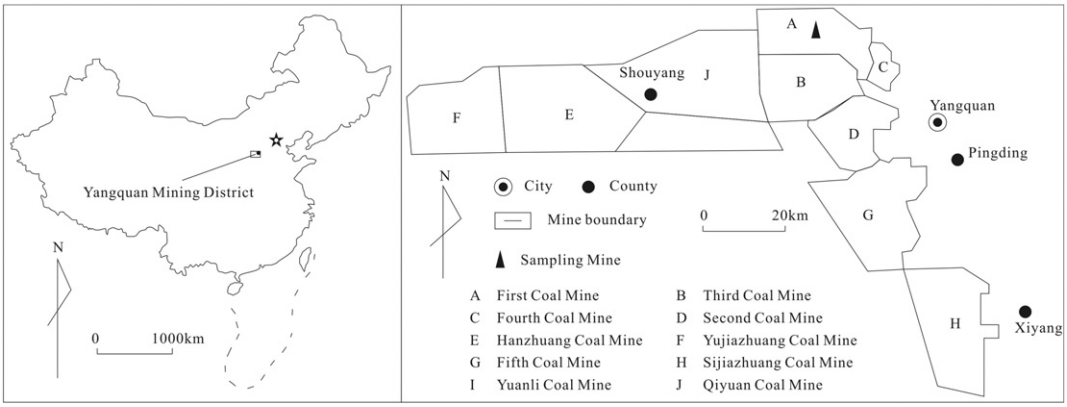


**Fig. 1.** Location of the Yangquan Mining District and sampling mine (Modified from Jiao and Wang, 1999)

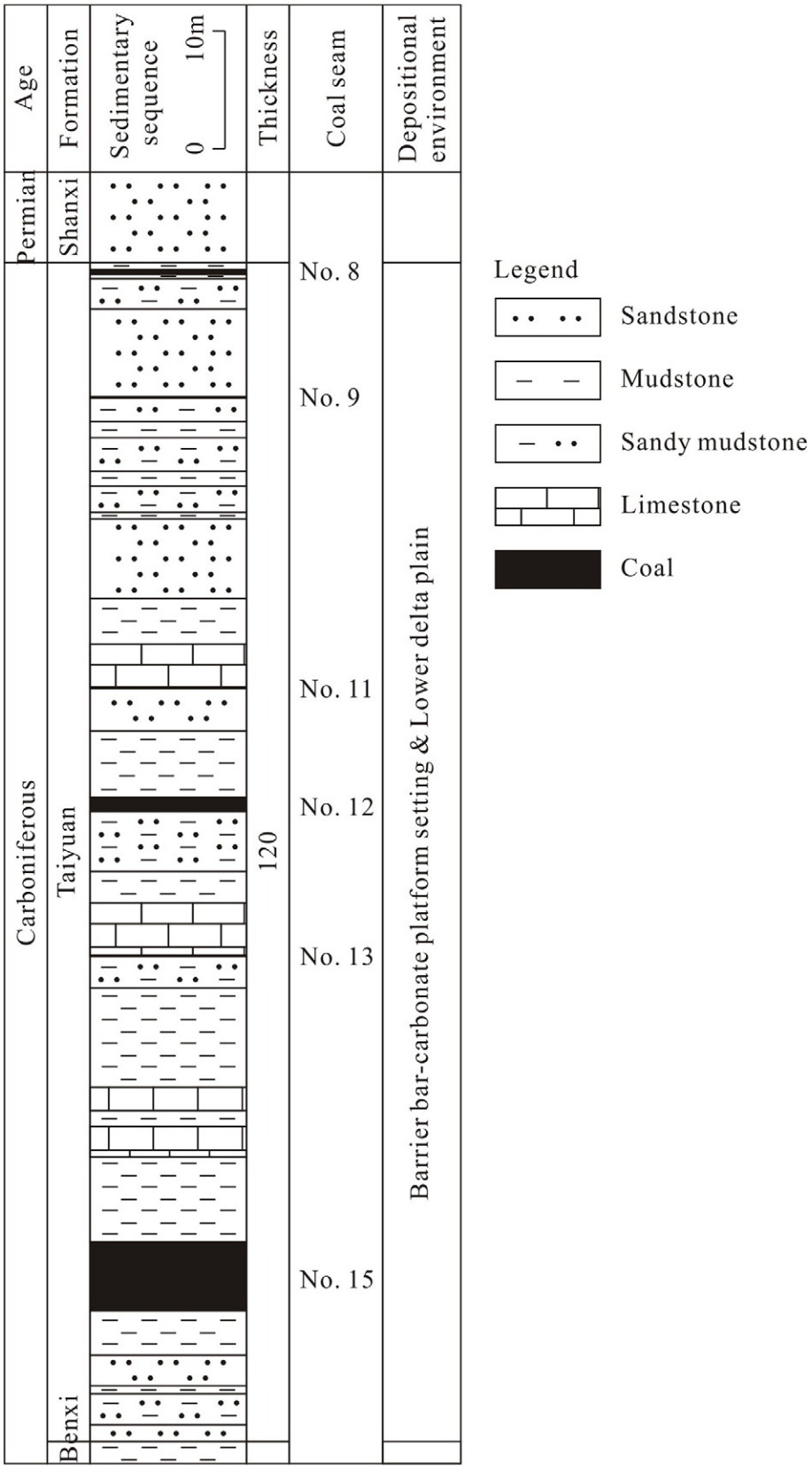


**Fig. 2.** Sedimentary sequence and depositional environment of the Yangquan Mining District (Modified from Jiao and Wang, 1999).

2010 (2010). The operating conditions for XRD analysis were as follows: power: 6 kW (40 kV, 150 mA); scanning speed: 4°/min; step: 0.02°; div slit: 1°; and rec slit: 0.3 mm. The XRD pattern was recorded over a 2θ interval of 4–45°. XRD analysis was performed by the State Key Laboratory of Coal Resources and Safe Mining, China University of Mining and Technology, Beijing.

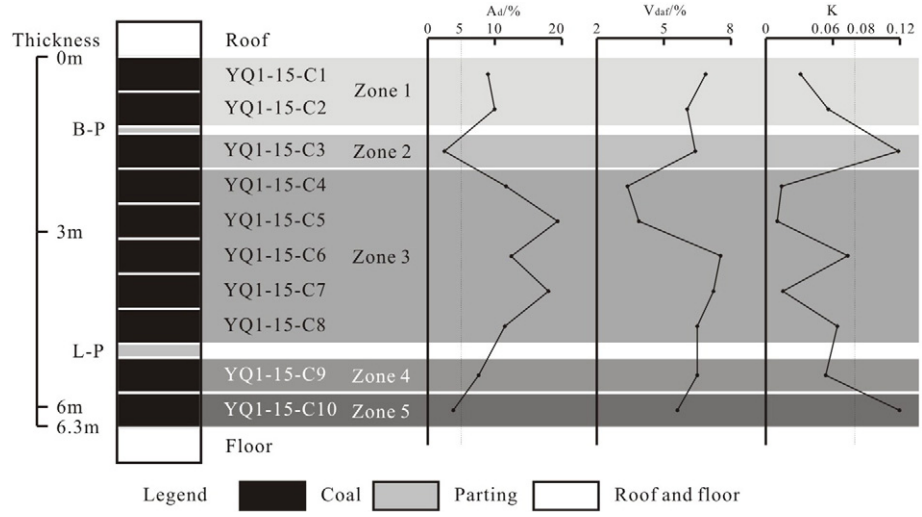


**Fig. 3.** Coal bench and parting samples, and vertical variations in $A_d$, $V_{daf}$ and K value.

### 3.4. X-ray fluorescence analysis

X-ray fluorescence (XRF; ARL ADVANT'XP+) spectrometry was used to determine the oxides of the major elements of the high-temperature ash (815 °C) of the coal and parting samples methods described by Dai et al. (2012a); these oxides include $SiO_2$, $TiO_2$, $Al_2O_3$, $Fe_2O_3$, MnO, MgO, CaO, $Na_2O$ and $K_2O$. The XRF analysis was performed by the State Key Laboratory of Coal Resources and Safe Mining, China University of Mining and Technology, Beijing.

### 3.5. Inductively coupled plasma mass spectrometry analysis

Inductively coupled plasma mass spectrometry (ICP-MS) was used to determine the contents of trace elements in the coal according to the method proposed by Dai et al. (2011) and Chinese Standard Method GB/T 14506.30-2010 (2011); these include Li, Be, Sc, V, Cr, Co, Ni, Cu, Zn, Ga, Rb, Sr, Y, Mo, Cd, In, Sb, Cs, Ba, La, Ce, Pr, Nd, Sm, Eu, Gd, Tb, Dy, Ho, Er, Tm, Yb, Lu, W, Tl, Pb, Bi, Th, and U. The ICP-MS analysis was performed by the China National Nuclear Corporation (CNNC) Beijing Research Institute of Uranium Geology.

## 4. Results

### 4.1. Coal chemistry

The volatile matter ($V_{daf}$) of the No. 15 Coal of Yangquan Mining District varies from 3.35% to 7.54% with a weighted average of 6.05% (Table 1). According to ASTM D 388-99 (2005), the Yangquan coal is an anthracite-grade coal, which is consistent with previous studies (Fu and Wu, 2012). The ash yield ($A_d$) of the No. 15 Coal varies from 2.55% to 19.41% with a weighted average of 10.61% (Table 1). According to the Chinese Standard Method GB/T 15224.1-2004 (2004), the Yangquan coal is an extra low- to medium-ash coal.

### 4.2. Minerals in coal

The minerals identified by XRD patterns of coal samples include kaolinite, ammonian illite, anatase, diaspore, calcite, dolomite, sodian illite, and quartz (Table 2; Fig. 4).

Ammonian illite and kaolinite are the dominate minerals, with mean proportions of 62.3% and 30.0%, respectively. Liu et al. (1996), Liang et al. (1996), and Dai et al. (2012a) identified ammonian illite in the coal seams of North China Coal Basin and suggested that this mineral was transformed from pre-existing kaolinite at a relatively high temperature (>150 °C). The inverse proportions of ammonian illite and kaolinite ($r = -0.98$) and the relatively high degree of coalification in the present study is compatible with the above suggestion.

Anatase and diaspore were identified in most coal samples with mean proportions of 0.8% and 2.1%, respectively. Diaspore has been identified in some Chinese coals (Dai et al., 2012a; Wang et al., 2011a, 2011b; Shi et al., 2014). This mineral is formed by gibbsite dehydration at a relatively high temperature, which is associated with igneous intrusions or a high degree of coalification (Permana et al., 2013).

**Table 1**
Sampling thickness (m), ash yield (%) and volatile matter (%) of coal benches collected from Yangquan Mining District.

| Sample | ST | $A_d$ | $V_{daf}$ |
|---|---|---|---|
| YQ1-15-C1 | 0.5 | 9.01 | 6.88 |
| YQ1-15-C2 | 0.5 | 10.01 | 6.07 |
| YQ1-15-C3 | 0.5 | 2.55 | 6.41 |
| YQ1-15-C4 | 0.5 | 11.65 | 3.35 |
| YQ1-15-C5 | 0.5 | 19.41 | 3.87 |
| YQ1-15-C6 | 0.5 | 12.45 | 7.54 |
| YQ1-15-C7 | 0.5 | 18.01 | 7.22 |
| YQ1-15-C8 | 0.5 | 11.51 | 6.50 |
| YQ1-15-C9 | 0.5 | 7.65 | 7.08 |
| YQ1-15-C10 | 0.5 | 3.89 | 5.61 |
| Av. | 0.5 | 10.61 | 6.05 |

ST, sampling thickness; $A_d$, ash yield; $V_{daf}$, volatile matter; Av., average value.

**Table 2**
Mineral compositions of coal benches determined applying X-ray diffraction and Quan and Softwares (%; on organic matter-free basis).

| Sample | Amm | Kao | An | Dia | Cal | Dol | Sod | Qua |
|---|---|---|---|---|---|---|---|---|
| YQ1-15-C1 | 50.3 | 40.4 | 0.2 | 2.9 | 1.2 | 5.0 | | |
| YQ1-15-C2 | 87.3 | 2.6 | 0.5 | 3.4 | 1.5 | 4.7 | | |
| YQ1-15-C3 | 92.4 | 7.6 | | | | | | |
| YQ1-15-C4 | 68 | 20.2 | 0.4 | 5.9 | 1.0 | | 4.5 | |
| YQ1-15-C5 | 77.6 | 19.5 | 2.2 | 0.7 | | | | |
| YQ1-15-C6 | 47.8 | 45.7 | 0.5 | | 6.0 | | | |
| YQ1-15-C7 | 72.9 | 22.1 | 2.3 | 2.7 | | | | |
| YQ1-15-C8 | 64.5 | 22.3 | 0.6 | 5.4 | 2.7 | | 4.5 | |
| YQ1-15-C9 | | 81.9 | 1.0 | | 1.6 | 4.6 | | 10.9 |
| YQ1-15-C10 | 62.2 | 37.8 | | | | | | |
| Av. | 62.3 | 30.0 | 0.8 | 2.1 | 1.4 | 1.4 | 1.0 | 1.1 |

Amm, ammonian illite; Kao, kaolinite; An, anatase; Dia, diaspore; Cal, calcite; Dol, dolomite; Sod, sodian illite; Qua, quartz; Av., average proportion.

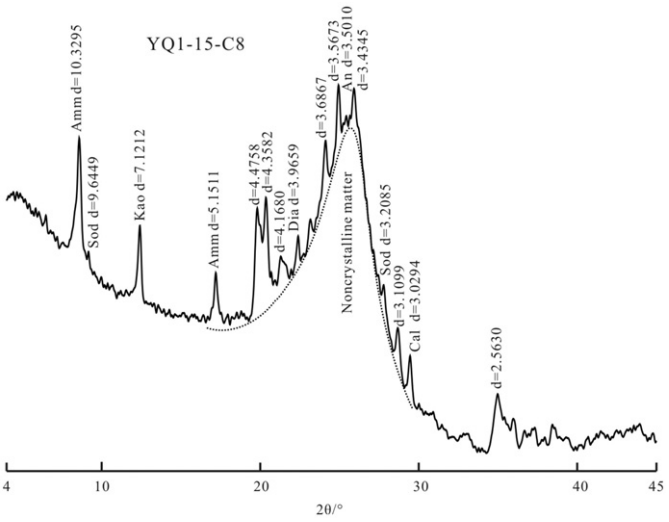


**Fig. 4.** Non-oriented XRD powder diffraction pattern of YQ1-15-C1 Amm, ammonian illite; Kao, kaolinite; An, anatase; Cal, calcite; Dol, dolomite; Dia, diaspore.

Alternatively, diaspore can be formed by Si-expulsion of kaolinite in weak reducing conditions (Shi et al., 2014; Zheng et al., 2016). In the present study, the diaspore is inferred to have been formed along with the conversion of kaolinite to ammonian illite.

Small proportions of calcite and dolomite, each with an average of 1.4%, were identified in some samples; however, the proportions of calcite in YQ1-15-C6 and dolomite in YQ1-15-C1 are as high as 6.0% and 5.0%, respectively. Carbonate minerals in coal are epigenetic minerals in common due to the acidic water of peat mire in the stage of peat accumulation, which has a positive effect on carbonate decomposition (Bouška et al., 2000; Dai et al., 2012a; Jiang et al., 2015; Belkin et al., 2010). Dai et al. (2012a) used XRD and SEM-EDX analyses to identify carbonate minerals in coal associated with igneous intrusions. Sutcu and Karayigit (2015) reported that calcite in coal is associated with fossil shells. In the current study, the calcite and dolomite in Yangquan coals are inferred to have been formed by epigenetic processes.

Small proportions of sodian illite were identified in YQ1-15-C4 and YQ1-15-C, each at 4.5%, which are considered to be associated with Na-rich volcanic ash input. Liang (1996) used an optical microscope to observed sodian illite associated with Na-rich volcanic ash in the Carboniferous coal from Third Coal Mine, which is adjacent to the sampling mine. Quartz was identified only in YQ1-15-C9, at 10.9%; however, ammonian illite is absent. This sample might have undergone stronger hydrodynamic forces than the other samples during peat accumulation.

### 4.3. Elements in coal

#### 4.3.1. Major element oxides

The contents of major element oxides in the Yangquan coal determined by XRF are shown in Table 3. Compared with Chinese coals, all of the major element oxides are depleted with a concentration coefficient (CC) <1, which is attributed mainly to the low ash yield for Yangquan coals (Fig. 5). Potassium oxide, MgO, CaO, $Fe_2O_3$, $P_2O_5$, and MnO are significantly depleted with CCs lower than 0.3; $Al_2O_3$, and $SiO_2$, and $TiO_2$ are depleted to some extent with CCs between 0.4 and 0.7. With a CC of 0.92, $Na_2O$ is close to the average value for Chinese coals, corresponding to the presence of sodian illite in some of the samples. The $SiO_2/Al_2O_3$ ratios of Yangquan coals, at an average of 1.25, are higher than those of kaolinite, tobelite, and paragonite at 1.18. This indicates that the $SiO_2/Al_2O_3$ ratios of ammonian illite and sodian illite are higher than 1.18, which is attributed mainly to the substitution of Si for Al in the tetrahedral sheets.

The $(CaO + MgO + Fe_2O_3)/(SiO_2 + Al_2O_3)$ ratio of coal (K value) can be used as an indicator of the depositional environment in the stage of peat accumulation when epigenetic processes are at a low level (Ren et al., 2006). Coal with a K value ≤0.22 is influenced mainly by fresh water during peat accumulation, and a ≥ 0.23 K value represents the influence of seawater. The K value of Yangquan coals varies from 0.011 to 0.120, with an average of 0.056, and is lower than 0.22. However, the relatively high total S content of the No. 15 Coal of Yangquan Mining District, at 2.3% on average, indicates that this coal was influenced by seawater during peat accumulation (Fu and Wu, 2012; Jiao and Wang, 1999). The K value of No. 15 Coal is lower than expected, which could be attributed to the relatively strong groundwater dynamic force, which results in the dissolution of some Ca- and Mg- bearing minerals in coal (e.g., calcite and dolomite). The strong correlation of K value and ash yield ($r = -0.82$) indicates that the coal is influenced by seawater (fresh water) when the ash yield is relatively low (high).

According to studies by Hayashi et al. (1997), He et al. (2010), and Dai et al. (2015a), the $Al_2O_3/TiO_2$ ratio can be used to indicate the parent rocks of sedimentary rocks and sediments in coal. Sedimentary rocks and sediments derived from mafic, intermediate, and felsic igneous rocks have $Al_2O_3/TiO_2$ ratios varying from 3 to 8, 8 to 21, and 21 to 70, respectively. The $Al_2O_3/TiO_2$ ratios of coal benches varying from 17.35 to 206.53 with an average of 66.42, indicate a parent material of felsic igneous rock. This is consistent with the Middle Proterozoic moyite of the Yinshan Old Land, which is a major source region of detrital materials for the North China Coal Basin (Dai et al., 2012b).

#### 4.3.2. Trace elements

The contents of trace elements in the coals collected from Yangquan Mining District are listed in Table 4. Compared with Chinese coals, most trace elements in Yangquan coals have a very low content with a CC <1,

**Table 3**
Contents of major element oxides and ratios of $SiO_2/Al_2O_3$, $(Fe_2O_3+CaO+MgO)/(SiO_2+Al_2O_3)$ and $Al_2O_3/TiO_2$ in coal benches (major element oxides in %; on whole-coal basis).

| Sample | $SiO_2$ | $Al_2O_3$ | $Na_2O$ | $K_2O$ | MgO | CaO | $Fe_2O_3$ | $TiO_2$ | MnO | $P_2O_5$ | $SiO_2/Al_2O_3$ | K | $Al_2O_3/TiO_2$ |
|---|---|---|---|---|---|---|---|---|---|---|---|---|---|
| YQ1-15-C1 | 3.96 | 3.19 | 0.16 | 0.006 | 0.077 | 0.148 | 0 | 0.015 | 0 | 0.0071 | 1.24 | 0.031 | 206.53 |
| YQ1-15-C2 | 4.47 | 3.60 | 0.26 | 0.005 | 0.054 | 0.327 | 0.073 | 0.044 | 0.0011 | 0.0156 | 1.24 | 0.056 | 82.67 |
| YQ1-15-C3 | 1.02 | 0.93 | 0.05 | 0.007 | 0.011 | 0.124 | 0.097 | 0.010 | 0.0012 | 0.0022 | 1.10 | 0.119 | 94.00 |
| YQ1-15-C4 | 5.64 | 4.51 | 0.21 | 0.021 | 0.020 | 0.081 | 0.045 | 0.054 | 0.0009 | 0.0099 | 1.25 | 0.014 | 83.89 |
| YQ1-15-C5 | 9.44 | 7.45 | 0.13 | 0.037 | 0.024 | 0.035 | 0.119 | 0.373 | 0.0005 | 0.0116 | 1.27 | 0.011 | 19.94 |
| YQ1-15-C6 | 5.68 | 4.47 | 0.16 | 0.021 | 0.022 | 0.514 | 0.214 | 0.102 | 0.0063 | 0.0056 | 1.27 | 0.073 | 43.82 |
| YQ1-15-C7 | 8.66 | 6.87 | 0.13 | 0.034 | 0.024 | 0.034 | 0.177 | 0.396 | 0.0003 | 0.0121 | 1.26 | 0.015 | 17.35 |
| YQ1-15-C8 | 5.22 | 4.25 | 0.22 | 0.019 | 0.048 | 0.318 | 0.245 | 0.080 | 0.0039 | 0.0100 | 1.23 | 0.064 | 53.20 |
| YQ1-15-C9 | 3.78 | 2.53 | 0.07 | 0.006 | 0.043 | 0.187 | 0.106 | 0.137 | 0.0011 | 0.0195 | 1.49 | 0.053 | 18.47 |
| YQ1-15-C10 | 1.80 | 1.56 | 0.06 | 0.012 | 0.009 | 0.027 | 0.367 | 0.035 | 0.0003 | 0.0046 | 1.16 | 0.120 | 44.33 |
| Av. | 4.97 | 3.94 | 0.14 | 0.017 | 0.033 | 0.179 | 0.144 | 0.124 | 0.0015 | 0.0098 | 1.25 | 0.056 | 66.42 |
| Chinese coal[a] | 8.47 | 5.89 | 0.16 | 0.19 | 0.22 | 1.21 | 4.85 | 0.33 | 0.015 | 0.092 | 1.44 | 0.437 | 17.85 |

K, $(Fe_2O_3+CaO+MgO)/(SiO_2+Al_2O_3)$.
[a] From Dai et al. (2012b)

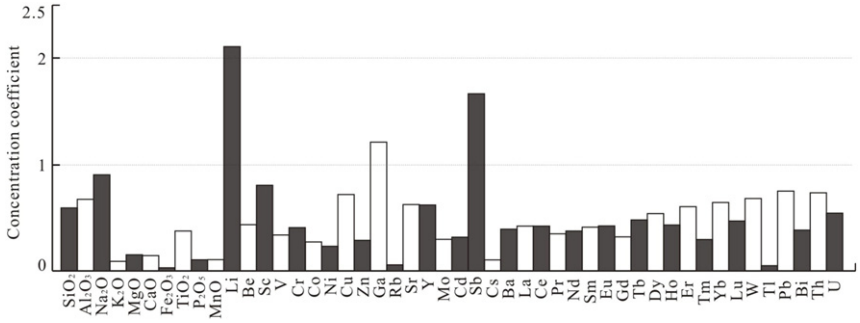


**Fig. 5.** The ratio of major element oxides and trace elements in coal bench samples of this study to Chinese coal. The concentration of major element oxides and trace elements in Chinese coal were cited from Dai et al. (2012b).

which is due mainly to the low ash yield. According to the classification levels of CC value proposed by Dai et al. (2015b), most elements including Be, V, Cr, Co, Ni, Zn, Mo, Cd, Cs, Ba, La, Ce, Pr, Nd, Sm, Eu, Gd, Tb, Tm, Lu, Tl, and Bi are significantly depleted with a CC <0.5, and Ga, Sb, Sc, Cu, Rb, Sr, Y, In, Dy, Ho, Er, Yb, W, Pb, Th, and U are close to the average values of Chinese coals with a CC ranging from 0.5 to 2, and only Li is slightly enriched with a CC of 2.1. No element is significantly enriched with a > 5 CC (Fig. 5).

**Table 4**
Concentrations of trace elements in coal benches and parting samples (trace elements in μg/g; on whole-coal basis).

| Sample | Li | Be | Sc | V | Cr | Co | Ni | Cu | Zn | Ga | Rb | Sr | Y |
|---|---|---|---|---|---|---|---|---|---|---|---|---|---|
| YQ1-15-C1 | 45.9 | 0.463 | 1.31 | 4.87 | 2.61 | 1.35 | 2.84 | 5.48 | 7.72 | 4.72 | 0.359 | 84.9 | 5.44 |
| YQ1-15-C2 | 57.6 | 0.449 | 2.85 | 5.78 | 3.88 | 0.695 | 1.69 | 10.2 | 4.33 | 3.31 | 0.181 | 156 | 7.18 |
| YQ1-15-C3 | 8.64 | 0.633 | 3.87 | 8.95 | 2.96 | 3.78 | 1.81 | 3.15 | 10.3 | 8.07 | 0.204 | 79.4 | 13.3 |
| YQ1-15-C4 | 83 | 0.544 | 1.4 | 5.69 | 2.5 | 1.39 | 1.54 | 4.66 | 9.93 | 7.16 | 0.604 | 80.8 | 5.75 |
| YQ1-15-C5 | 136 | 1.060 | 5.82 | 19.2 | 9.8 | 0.794 | 1.91 | 26.9 | 14.2 | 11.1 | 0.986 | 68.8 | 14.4 |
| YQ1-15-C6 | 79.7 | 0.584 | 5.13 | 15.1 | 6.72 | 1.25 | 2.35 | 14.7 | 13.2 | 9.15 | 0.642 | 78.2 | 10.3 |
| YQ1-15-C7 | 114 | 0.881 | 5.67 | 20.4 | 9.49 | 0.833 | 1.98 | 32.9 | 11.6 | 10.7 | 0.862 | 67.9 | 13.2 |
| YQ1-15-C8 | 99.3 | 0.759 | 1.87 | 10.4 | 4.8 | 2.26 | 2.44 | 10.7 | 12.6 | 10.8 | 0.676 | 110 | 6.57 |
| YQ1-15-C9 | 27.8 | 0.948 | 5.54 | 22.2 | 15.9 | 2.35 | 2.51 | 12.4 | 12.8 | 10.9 | 0.209 | 103 | 19.9 |
| YQ1-15-C10 | 18.3 | 2.810 | 1.72 | 4.15 | 3.62 | 4.26 | 12.7 | 3.85 | 24.2 | 3.33 | 0.362 | 43.3 | 16.3 |
| Av. | 67.0 | 0.913 | 3.52 | 11.67 | 6.23 | 1.896 | 3.18 | 12.49 | 12.09 | 7.92 | 0.509 | 87.2 | 11.23 |
| Chinese coal[a] | 31.8 | 2.11 | 4.38 | 35.1 | 15.4 | 7.08 | 13.7 | 17.5 | 41.4 | 6.55 | 9.25 | 140 | 18.2 |
| Bacunshi-P | 41.8 | 1.73 | 11.7 | 53.4 | 43.2 | 2.6 | 9.29 | 29.1 | 15.3 | 19.9 | 26.4 | 217 | 24.5 |
| Lvshi-P | 247 | 2.69 | 6.72 | 10.4 | 3.33 | 0.443 | 0.739 | 4.64 | 9.33 | 31.7 | 10.8 | 114 | 10.2 |

| | Mo | Cd | In | Sb | Cs | Ba | La | Ce | Pr | Nd | Sm | Eu | Gd |
|---|---|---|---|---|---|---|---|---|---|---|---|---|---|
| YQ1-15-C1 | 0.863 | 0.149 | 0.016 | 12.9 | 0.082 | 47.5 | 5.08 | 11 | 1.24 | 4.36 | 0.827 | 0.174 | 0.818 |
| YQ1-15-C2 | 0.634 | 0.067 | 0.029 | 0.14 | 0.097 | 85.2 | 10.6 | 22.7 | 2.61 | 9.26 | 1.9 | 0.373 | 1.6 |
| YQ1-15-C3 | 0.695 | 0.064 | 0.02 | 0.123 | 0.056 | 26.6 | 0.118 | 0.307 | 0.056 | 0.46 | 0.454 | 0.176 | 0.495 |
| YQ1-15-C4 | 0.884 | 0.063 | 0.023 | 0.071 | 0.144 | 72.2 | 13.1 | 25.6 | 2.96 | 10.8 | 1.83 | 0.318 | 1.54 |
| YQ1-15-C5 | 1.23 | 0.047 | 0.084 | 0.114 | 0.195 | 94.4 | 14.5 | 30.9 | 3.54 | 13 | 2.46 | 0.592 | 2.14 |
| YQ1-15-C6 | 0.774 | 0.048 | 0.04 | 0.105 | 0.147 | 57.8 | 8.17 | 18.2 | 2.17 | 8.01 | 1.8 | 0.352 | 1.6 |
| YQ1-15-C7 | 1.13 | 0.076 | 0.083 | 0.103 | 0.185 | 92 | 14.3 | 30.8 | 3.36 | 12.4 | 2.46 | 0.584 | 2.08 |
| YQ1-15-C8 | 1.34 | 0.034 | 0.028 | 0.295 | 0.13 | 69.7 | 11 | 22.8 | 2.59 | 9.1 | 1.65 | 0.283 | 1.42 |
| YQ1-15-C9 | 0.917 | 0.098 | 0.031 | 0.068 | 0.071 | 31.2 | 8.53 | 16.3 | 1.93 | 7.15 | 1.56 | 0.382 | 1.49 |
| YQ1-15-C10 | 0.553 | 0.155 | 0.014 | 0.105 | 0.042 | 41.8 | 8.98 | 16.7 | 1.98 | 7.88 | 1.67 | 0.304 | 1.55 |
| Av. | 0.902 | 0.080 | 0.037 | 1.402 | 0.115 | 61.8 | 9.438 | 19.531 | 2.244 | 8.24 | 1.661 | 0.354 | 1.473 |
| Chinese coal[a] | 3.08 | 0.25 | 0.047 | 0.84 | 1.13 | 159 | 22.5 | 46.7 | 6.42 | 22.3 | 4.07 | 0.84 | 4.65 |
| Bacunshi-P | 1.54 | 0.113 | 0.123 | 0.109 | 3.11 | 493 | 78.3 | 152 | 16.5 | 59.8 | 10.2 | 1.87 | 9.59 |
| Lvshi-P | 1.96 | 0.053 | 0.052 | 0.178 | 1.3 | 365 | 24.6 | 48.8 | 5.36 | 18.5 | 2.87 | 0.537 | 2.73 |

| | Tb | Dy | Ho | Er | Tm | Yb | Lu | W | Tl | Pb | Bi | Th | U |
|---|---|---|---|---|---|---|---|---|---|---|---|---|---|
| YQ1-15-C1 | 0.17 | 1.07 | 0.21 | 0.534 | 0.095 | 0.662 | 0.085 | 0.879 | 0.028 | 7.99 | 0.117 | 1.82 | 0.543 |
| YQ1-15-C2 | 0.285 | 1.56 | 0.294 | 0.75 | 0.122 | 0.833 | 0.105 | 0.176 | 0.007 | 5.89 | 0.155 | 2.4 | 0.564 |
| YQ1-15-C3 | 0.193 | 1.96 | 0.483 | 1.28 | 0.274 | 1.98 | 0.279 | 2.55 | 0.009 | 1.41 | 0.051 | 0.458 | 0.505 |
| YQ1-15-C4 | 0.25 | 1.26 | 0.237 | 0.651 | 0.104 | 0.727 | 0.095 | 0.736 | 0.014 | 5.12 | 0.159 | 2.25 | 0.686 |
| YQ1-15-C5 | 0.431 | 2.75 | 0.552 | 1.43 | 0.252 | 1.75 | 0.232 | 0.587 | 0.022 | 31.3 | 0.882 | 13.9 | 2.93 |
| YQ1-15-C6 | 0.358 | 2.37 | 0.468 | 1.14 | 0.207 | 1.39 | 0.18 | 0.219 | 0.011 | 7.06 | 0.222 | 4.38 | 2.05 |
| YQ1-15-C7 | 0.39 | 2.5 | 0.524 | 1.38 | 0.232 | 1.68 | 0.223 | 0.509 | 0.022 | 33.4 | 0.946 | 11.8 | 2.97 |
| YQ1-15-C8 | 0.232 | 1.28 | 0.257 | 0.714 | 0.11 | 0.778 | 0.105 | 0.697 | 0.017 | 10.9 | 0.225 | 2.31 | 1.26 |
| YQ1-15-C9 | 0.382 | 3.2 | 0.716 | 1.84 | 0.357 | 2.44 | 0.322 | 0.423 | 0.011 | 3.22 | 0.174 | 3.09 | 1.64 |
| YQ1-15-C10 | 0.305 | 2.03 | 0.441 | 1.07 | 0.168 | 1.13 | 0.146 | 0.569 | 0.077 | 7.17 | 0.082 | 0.732 | 0.223 |
| Av. | 0.300 | 2.00 | 0.418 | 1.08 | 0.192 | 1.34 | 0.177 | 0.735 | 0.022 | 11.35 | 0.301 | 4.314 | 1.337 |
| Chinese coal[a] | 0.62 | 3.74 | 0.96 | 1.79 | 0.64 | 2.08 | 0.38 | 1.08 | 0.47 | 15.1 | 0.79 | 5.84 | 2.43 |
| Bacunshi-P | 1.36 | 5.7 | 1.04 | 2.96 | 0.407 | 2.87 | 0.387 | 1.74 | 0.207 | 23.7 | 0.578 | 20.7 | 4.38 |
| Lvshi-P | 0.437 | 2.22 | 0.413 | 1.12 | 0.185 | 1.27 | 0.173 | 3.58 | 0.827 | 6.65 | 1.09 | 23.5 | 6.99 |

[a] From Dai et al. (2012b)

## 5. Discussion

### 5.1. Vertical variations

Each coal bench has different mineral assemblages, ash yields and K values, indicating different local geochemical conditions. According to the method proposed by Dai et al. (2006) and the vertical variations in mineral assemblages, ash yields, and K values, the No. 15 Coal of Yangquan Mining District is divided into the following five zones (Fig. 3).

Zone 1: This zone includes YQ-15-C1 and YQ-15-C2 benches. The minerals are dominated by ammonian illite and kaolinite, at >10%, with small proportions of dolomite, diaspore, anatase, and calcite at <10%. The relatively high ash yield, at 9.5%, and the low K value of 0.04 indicate that this zone was influenced mainly by both seawater and fresh water during peat accumulation. Antimony is significantly enriched with a CC of 7.76, and Li is somewhat enriched with a CC of 1.62 in this zone.

Zone 2: This zone is YQ1-15-C3 Bench. The proportion of ammonian illite in this bench is as high as 92.4%, and kaolinite has a small proportion of 7.6%. No other minerals with small proportions were identified, which is attributed mainly to the relatively low ash. The relatively low ash yield, at 2.5%, and high K value of 0.12 indicate that this zone was influenced mainly by seawater during peat accumulation. In this zone, Ga and W are enriched to some extent.

Zone 3: This zone includes YQ1-15-C4, YQ1-15-C5, YQ1-15-C6, YQ1-15-C7, and YQ1-15-C8 benches. The minerals are dominated by ammonian illite and kaolinite, at >10%, with small proportions of anatase, diaspore, calcite, dolomite, and sodian illite, at <10%. The relatively high ash yield, at 14.6%, and low K value of 0.04 indicate that this zone was influenced mainly by both seawater and fresh water during peat accumulation. In this zone, $Na_2O$, Li, Cu, Ga, In, Pb, and Th are enriched with a CC >1, which is attributed mainly to the relatively high ash yield and the Na-rich volcanic ash input.

Zone 4: This zone is YQ1–15-C9 Bench. The minerals are dominated by kaolinite and quartz, at >10%, with small proportions of anatase, calcite, and dolomite at <10%. Ammonian illite is absent in this zone, which is different from the other zones. The relatively high ash yield, at 7.7%, and the low K value of 0.05 indicate that this zone was influenced by both seawater and fresh water during peat accumulation.

Zone 5: This zone is YQ1-15-C10 Bench. The minerals are dominated by ammonian illite and kaolinite, at >10%. No other minerals with low proportions were identified, which is due mainly to the relatively low ash. This zone is characterized by low ash, at 3.9%, and a high K value of 0.12, which indicates the influence of mainly seawater during peat accumulation.

Clay minerals are sensitive to ambient conditions; thus, clay mineral assemblages can act as indicators of depositional environments (Zhao and Zhang, 1990; Xu et al., 2003). According to the previous discussions, Zones 2 and 5 were influenced mainly by seawater during peat accumulation and have an average ammonian illite/kaolinite (Am/Kao) value of 6.9. This value is higher than that of Zones 1, 3, and 4, with an average Am/Kao value of 6.3, indicating the influence of mainly fresh water and seawater. This indicates that compared with fresh water, seawater is more favorable for the conversion of kaolinite to ammonian illite in coal during coalification. This is likely attributed to the relatively high pH and reducing conditions of seawater.

### 5.2. Comparison of XRD and XRF analyses

According to the method proposed by Ward et al. (1999) and Dai et al. (2012a), the inferred proportions of $SiO_2$, $Al_2O_3$, $K_2O$, $Na_2O$, $TiO_2$, CaO, and MgO were calculated from Quan software results. This method includes the loss of hydroxyl water from clay and bauxite minerals, $CO_2$ from carbonates, and $NH_3$ from ammonian illite, which are released totally from the corresponding minerals at temperatures as high as 815 °C (Liu et al., 2009). The chemical formulae of kaolinite, anatase, diaspore, calcite, dolomite, sodian illite, and quartz used in the calculation are listed as follows: $Al_4Si_4O_{10}(OH)_8$, $TiO_2$, AlO(OH), $CaCO_3$, $(Ca,Mg)(CO_3)_2$, $NaAl_2(Al,Si_3)O_{10}(OH)_2$, and $SiO_2$. As described by Zheng et al. (2016), Higashi (2000), and Zhao and Zhang (1990), the chemical formula of ammonian illite used in the present study is $(NH_{4x},K_{1-x})Al_2(Al,Si_3)O_{10}(OH)_2$, which is the solid solution between muscovite and tobelite. The $x$ for each sample was calculated according to the method described by Drits et al. (1997):

$$NH_4/(NH_4+K) = 2.786d_{001} - 27.79. \quad (1)$$

The XRF data, including $SiO_2$, $Al_2O_3$, $K_2O$, $Na_2O$, $TiO_2$, CaO, MgO, $Fe_2O_3$, and MnO were also normalized for comparison with the XRD data.

The proportions of $SiO_2$, $Al_2O_3$, $K_2O$, $Na_2O$, $TiO_2$, CaO, and MgO inferred from the XRD data were compared graphically with those normalized from the XRF data; these two sets of proportions are shown as X–Y plots with a diagonal line in Fig. 6.

The points for $SiO_2$ and $Al_2O_3$ plots fell above and below the diagonal lines, indicating that those inferred from the XRD data are lower and higher than those normalized from the XRF data, respectively. This occurred because the $Si/Al^{IV}$ ratio of the tetrahedral sheets in ammonian illite was considered to be 3 for the calculation of $SiO_2$ and $Al2O_3$ proportions from XRD data; however, the actual $Si/Al^{IV}$ ratio of the current ammonian illite is higher than 3. In the process from coalification to low-grade metamorphism, ammonian illite would gradually be transformed to tobelite, muscovite, or the solid solution between them, along with the expulsion of Si from the tetrahedral sheets, the integration of Al into the tetrahedral sheets, and an $Si/Al^{IV}$ ratio approaching 3.

The points for $Na_2O$ and CaO plots fell above the diagonal lines, indicating lower proportions of $Na_2O$ and CaO inferred from the XRD data compared with those normalized from the XRF data. This is mainly attributed to the interlay cations of ammonian illite dominated by $NH_4^+$ and $K^+$ that contain some amount of $Ca^{2+}$ and $Na^+$.

No dolomite was identified in most samples by XRD, although these samples have a < 0.5% MgO proportion normalized from the XRF data. This is attributed mainly to the low content of dolomite below the XRD detection limit or the substitution of some amount of $Al^{VI}$ in the octahedral sheets of ammonian illite by Mg. The points representing YQ1-15-C1, YQ1-15-C2, and YQ1-15-C9 for the MgO plot, which contain some proportions of dolomite at 5%, 4.7%, and 4.6%, respectively, fell below the diagonal line. This indicates higher MgO proportions inferred from the XRD data than those normalized from the XRF data. This result is likely attributed to the isomorphous substitution of Mg in dolomite by Fe; the dolomite in the present study was inferred to be the solid solution between dolomite and ankerite.

The points for the $K_2O$ plot were scattered to some extent, which is attributed mainly to the relatively low proportion of $K_2O$. In addition, the isomorphous substitution of Al for Si in the tetrahedral sheets and the integration of $Na^+$ and $Ca^{2+}$ have significant effects on the $K^+$ proportion within the total interlayer cations of ammonian illite, resulting in the scattered $K_2O$ plot.

The points for the $TiO_2$ plot were scattered but were still parallel to the equality line, indicating that Ti occurs mainly as anatase.

No Fe-bearing mineral was identified in Yangquan coal, although some proportion of $Fe_2O_3$ was still detected by XRF. This is attributed to the content of pyrite, a common Fe-dominated mineral in coal below the XRD detection limit. In addition, some Fe may have been substituted for $Al^{VI}$ in the ammonian illite.

### 5.3. Cluster analysis

Cluster analysis was used in the present study to identify the organic or inorganic affinity of major element oxides and trace elements in the Yangquan coal. According to the results of this analysis, the major

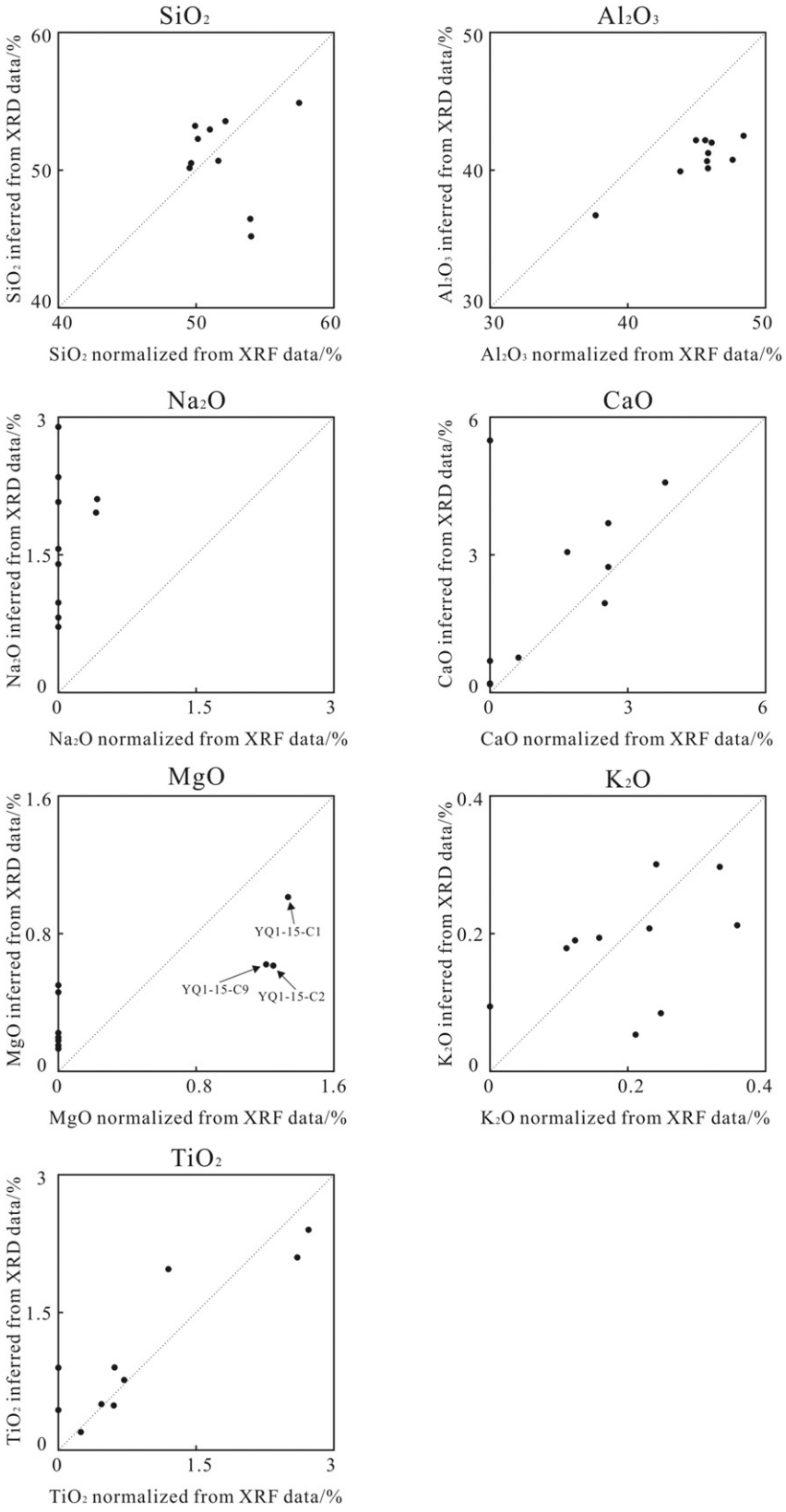


**Fig. 6.** Comparisons between major element oxides inferred from XRD data and those normalized from XRF data.

element oxides and trace elements were divided into four groups, each of which is described in Fig. 7.

Group 1 includes $SiO_2$, $Al_2O_3$, $TiO_2$, Li, Cs, $K_2O$, Rb, Ba, Pb, Ce, Pr, La, Nd, Sm, Gd, Eu, Tb, Cu, U, In, Th, and Bi. All of these elements have correlation coefficients with ash yields higher than 0.75 except for Tb, which has a relatively low correlation coefficients with ash yield but is as high as 0.61. These elements have strong inorganic affinity and occur mainly in silicate or aluminosilicate minerals such as kaolinite and ammonian illite. In this group, most elements are lithophile elements except for Cu, Pb, In, and Bi (Liu et al., 1984). Copper is a typical

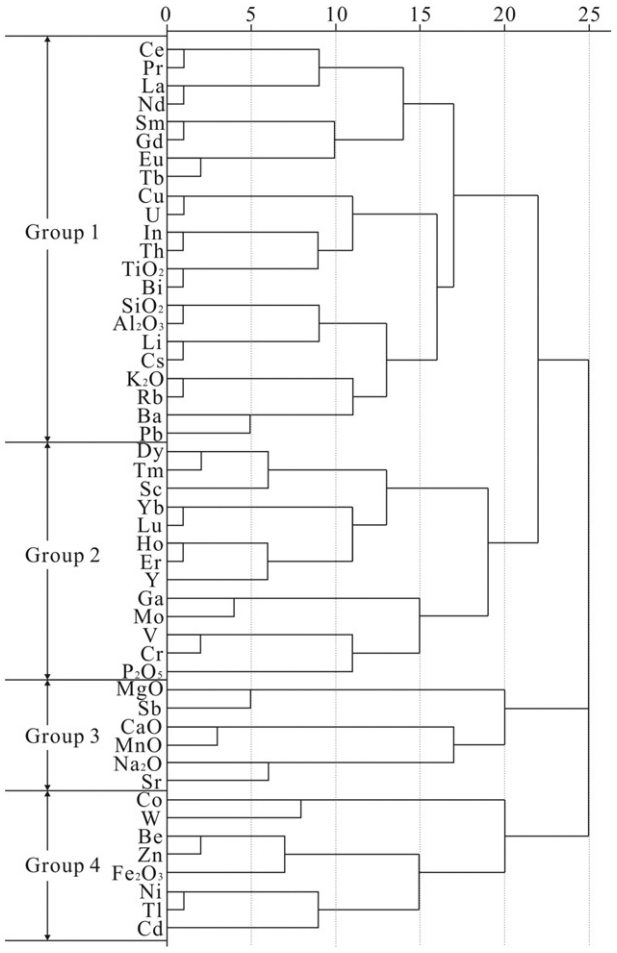


**Fig. 7.** Dendrogram produced by cluster analysis of analytical results for 10 coal bench samples.

chalcophile element and occurs mainly as sulfide in reducing conditions; thus, Cu in the present study is inferred to occur as a sulfide inclusion or ultramicro inclusion in clay minerals. Indium and Bi have strong correlations with Cu ($r_{Cu-In} = 0.97$, $r_{Cu-Bi} = 0.97$), indicating similar modes of occurrences as Cu. Lead is a chalcophile element and occurs mainly as sulfide in coal. However, $Pb^{2+}$ can isomorphously substitute for $K^+$ in endogenic conditions owing to their similar charges and cation radii (Liu et al., 1984). The Pb in Yangquan coal is inferred to have substituted for the interlayer $K^+$ of ammonian illite owing to the strong correlation between $K_2O$ and Pb ($r_{Pb-K_2O} = 0.87$).

Group 2 includes $P_2O_5$, Dy, Tm, Sc, Yb, Lu, Ho, Er, Y, Ga, Mo, V and Cr. With the exception of Mo, Ga, and V, these elements have relatively weak correlations with ash yield, with correlation coefficients varying from −0.14 to 0.46; this indicating both organic and inorganic affinity. The heavy REYs (HREYs) and several medium REYs (MREYs) in Yangquan coal are associated with organic matter to some extent. Gallium is typical dispersed element and generally substitutes for Al occurring in aluminum hydroxide minerals or clay minerals (Dai et al., 2006, 2012a, 2012c; Shi et al., 2014; Ren et al., 2006). Compared with the lithophile elements in Group 1, the Ga in Yangquan coal is less strongly correlated with ash yield ($r_{Ga-ash} = 0.53$) and is weakly correlated with diaspore ($r_{Ga-diaspore} = 0.06$). This indicates that Ga substitutes for Al occurring in clay minerals and also in organic matter to some extent. The Ga is enriched in Zones 2, 3, and 4 to some extent. However, the $Al_2O_3$ is depleted in these three zones, indicating that the Ga in the organic fraction has different origins from that in the inorganic fraction, such as coal-forming plants and depositional water. The V in Yangquan coal has a similar mode of occurrence as Ga owing to their similar correlation coefficients with ash yield. The Mo in Yangquan coal has a correlation coefficient of 0.71 with ash yield, indicating that Mo occurs mainly in clay minerals and to a small extent in organic matter. The mode of occurrence of Mo in the inorganic fraction is inferred to be similar to that of Cu owing to its chalcophile properties, and the Mo in the organic fraction is inferred to be derived from coal-forming plants because this element is essential for plants (Liu et al., 1984).

Group 3 includes MgO, CaO, $Na_2O$, MnO, Sb, and Sr. This group represents the elements occurring in carbonate minerals, although it has a weak correlation with ash yield ($r_{ash}$ from −0.10 to 0.08). The MnO in Yangquan coal is strongly correlated with CaO ($r_{CaO-MnO} = 0.87$) but weakly correlated with $Fe_2O_3$ ($r_{Fe_2O_3-MnO} = 0.32$), indicating that the Mn occurs mainly as carbonate rather than sulfide. Antimony is a chalcophile element and occurs generally as sulfide in coal. In the current study, Sb in Yangquan coal is strongly correlated with MgO ($r_{Sb-MgO} = 0.71$) but negatively correlated with $Fe_2O_3$ ($r_{Sb-Fe_2O_3} = -0.46$), indicating that the Sb occurs mainly in dolomite rather than sulfide. The Sb in the YQ1-15-C1 Bench is significantly enriched (CC = 14.0) and is inferred to be associated with leaching of the overlying floor by groundwater. The mode of occurrence of Sb in the Yangquan coal requires further study.

Group 4 includes $Fe_2O_3$, Co, W, Be, Zn, Ni, Tl, and Cd. Most elements in this group are chalcophile elements. Zinc, Ni, and Tl are weakly but negatively correlated with ash yield ($r_{ash}$ from −0.45 to −0.17) and are positively correlated with $Fe_2O_3$ strongly ($r_{Fe_2O_3}$ from 0.65 to 0.83), indicating the occurrence of sulfide. Although weakly correlated with $Fe_2O_3$, the Cd is relatively strongly correlated with Ni and Tl ($r_{Cd-Ni} = 0.68$, $r_{Cd-Tl} = 0.71$), also indicating a sulfide occurrence. The Co is strongly negatively correlated with ash yield ($r_{Co-ash} = -0.82$), indicating an organic affinity, and the W in Yangquan coal is less strongly correlated with ash yield ($r_{W-ash} = -0.50$), indicating a dominant organic affinity followed by inorganic affinity. Beryllium is a lithophile element and occurs mainly in silicate or aluminosilicate in coal. In the present study, Be has strongly positive correlation with $Fe_2O_3$; its mode of occurrence requires further study.

### 5.4. Rare earth elements and yttrium

The total REY content of Yangquan coal varies from 21.815 μg/g to 88.929 μg/g with an average weight of 59.677 μg/g. This value is significantly lower than that of Chinese coal, at 135.89 μg/g, owing mainly to the low ash yield. Zones 1, 3, and 4, influenced by both fresh water and seawater during peat accumulation, have a mean total REY content of 64.288 μg/g. This value is higher than the average value of 41.235 μg/g for Zones 2 and 5, which were influenced by seawater during peat accumulation. According Seredin and Dai (2012) and Dai et al. (2016), a threefold classification of REY was used for this study: light REY (LREY), including La, Ce, Pr, Nd, and Sm; MREY, including Eu, Gd, Tb, Dy, and Y; and HREY, including Ho, Er, Tm, Yb, and Lu. According to the correlation of ash yield with various REYs, the inorganic affinity of REY is shown in order as LREY > MREY > HREY. The LREY, Eu, Gd, and Tb in Yangquan coal are characterized by inorganic affinity, and HREY, Dy, and Y are characterized by both organic and inorganic affinities. Compared with the upper continental crust (UCC) in North China, two REY enrichment types were identified for Yangquan coal: light (L)-type REY enrichment ($La_N/Lu_N > 1$) and heavy (H)-type REY enrichment ($La_N/Lu_N < 1$). The REY distribution patterns for coal benches are shown in Fig. 8. Zones 1, 3, and 5 are characterized by L-type distribution with $La_N/Lu_N$ values of 1.51, 1.56, and 1.15, respectively, and zones 2 and 4 are characterized by H-type distribution with $La_N/Lu_N$ values of 0.008 and 0.50, respectively. Compared with coal benches, Baicunshi and Lvshi Partings have a significantly LREY-enriched distribution pattern with $La_N/Lu_N$ values of 3.79 and 2.67, respectively. The L-type distributions and Eu minimums (δEu), in Zones 1, 3, and 5, at 0.66, 0.6, and 0.58, respectively, indicate terrigenous origin (Seredin and Dai, 2012;

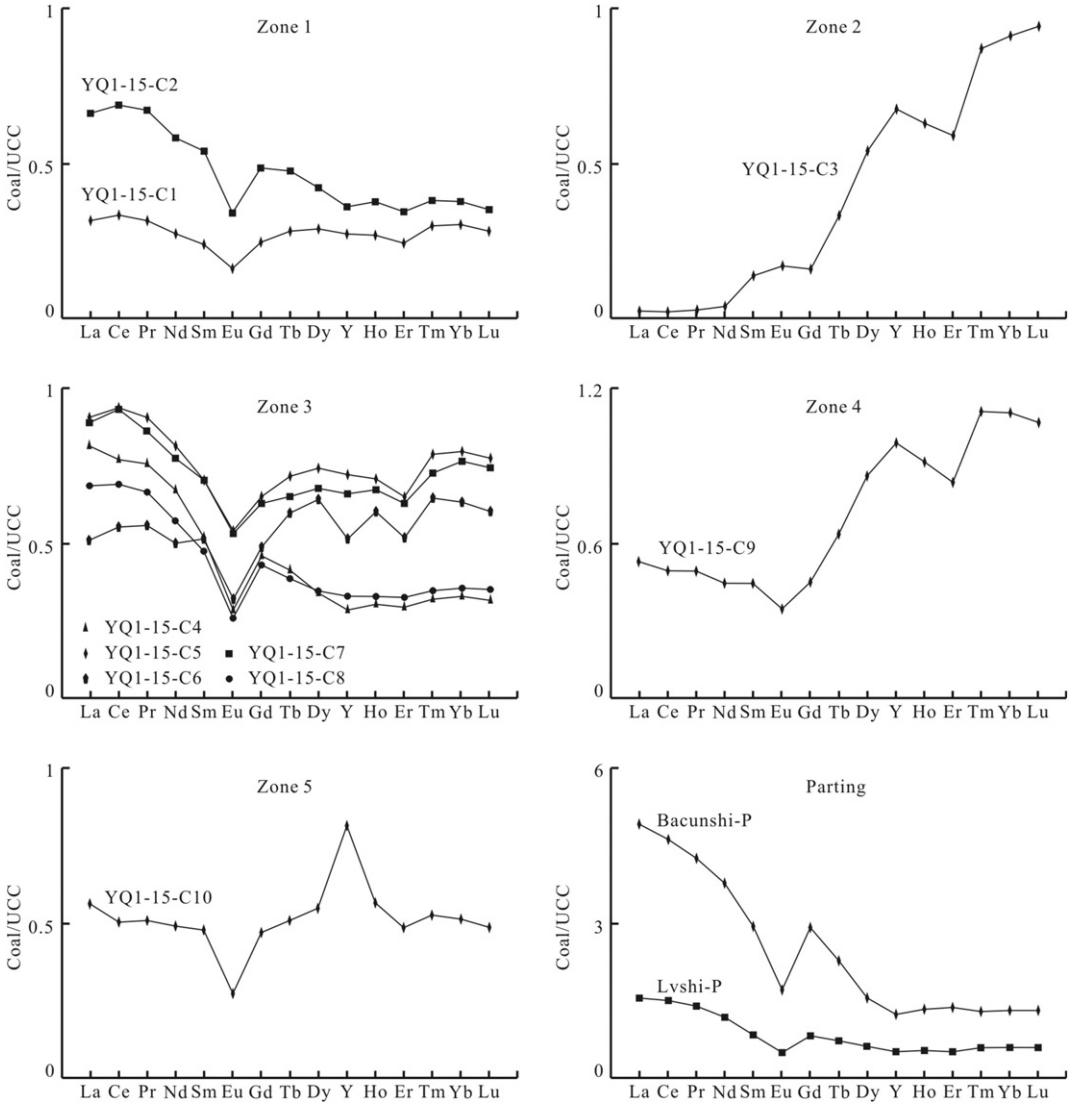


**Fig. 8.** REY distribution patterns of coal bench and parting samples normalized by Upper Continental Crust (UCC) of North China. The REY concentrations of UCC were cited from Chi and Yan (2007).

Dai et al., 2012c), and The H-type distribution and δEu, 1.14 and 0.77, respectively, are higher than those of Zones 1, 3, and 5. This indicates an origin different from terrigenous detritals for REY, particularly for HREY in Zones 2 and 4. These zones closely underlie Bacunshi and Lvshi Parting, which are characterized by significant HREY enrichment. As described by Dai et al. (2014, 2016), the leaching of overlying partings by groundwater during parting formation resulted in the H-type distribution for Zones 2 and 4. The δCe of Zones 2 and 5, at 0.85 and 0.95, respectively, is lower than those of Zones 1, 3, and 4, at 1.04, 1.03, and 0.96, respectively. These results are compatible with the influences of Zones 2 and 5 by seawater and Zones 1, 3, and 4 by both seawater and fresh water.

## 6. Conclusion

The Yangquan coal is an anthracite coal characterized by low $A_d$ and $V_{daf}$, with average values of 10.61% and 6.05%, respectively. Almost all of the major element oxides and trace elements are depleted in this coal compared with other Chinese coal, which is attributed mainly to low $A_d$. The minerals in Yangquan coal are dominated by ammonian illite and kaolinite, followed by calcite, dolomite, anatase, sodian illite, and diaspore.

The mineral assemblages, $A_d$, and K values of the coal bench samples vary significantly in the vertical direction. The coal influenced by seawater during peat accumulation is characterized by low ash, a high K value, and a high proportion of ammonian illite.

The major element oxides and trace elements in the coal bench samples were divided into four groups according to cluster analysis. Group 1, represented by $SiO_2$ and $Al_2O_3$, occurs mainly in silicate or aluminosilicate minerals. Group 2, represented by HREY, is characterized by both organic and inorganic affinities. Group 3, represented by MgO and CaO, occurs mainly in carbonate minerals. Group 4, represented by $Fe_2O_3$, occurs mainly in sulfide minerals.

The Yangquan coal is characterized by L-type REY distribution and <1 δEu, indicating an terrigenous detrital origin. Zone 2 and Zone 4 are characterized by H-type REY distribution attributed mainly to leaching of the overlying partings.

## Acknowledgments

This research was supported by the National Natural Science Foundation of China (Nos. 41502154 and 41072119), the Coal Seam Gas Joint Research Fund of Shanxi Province (No. 2013012005), the Technological Key Research Program of Education Department Henan Province (No.

13A170011), and Doctor Foundation of Henan Institute of Engineering (No. D2013016).

## References


Ali, J., Kazi, T.G., Baig, J.A., Afridi, H.I., Arain, M.S., Ullah, N., Arain, S.S., Siraj, S., 2015. Monitoring of arsenic fate with proximate parameters and elemental composition of coal from Thar coalfield, Pakistan. J. Geochem. Explor. 159, 227–233.

ASTM D 388-99, 2005. Annual Book of ASTM Standards. Standard Classification of Coals by Rank: Gaseous Fuels; Coal and Coke, Vol. 05.06.

ASTM D3174-04, 2005. Annual Book of ASTM Standards. Test Method for Ash in the Analysis Sample of Coal and Coke From Coal: Gaseous Fuels; Coal and Coke, Vol. 05.06.

ASTM D3175-02, 2005. Annual Book of ASTM Standards. Test Method for Volatile Matter in the Analysis Sample of Coal and Coke: Gaseous Fuels; Coal and Coke, Vol. 05.06.

Belkin, H.E., Tewalt, S.J., Hower, J.C., Stucker, J.D., O'Keefe, J.M.K., Tatu, C.A., Buia, G., 2010. Petrography and geochemistry of Oligocene bituminous coal from the Jiu Valley, Petroşani basin (southern Carpathian Mountains), Romania. Int. J. Coal Geol. 82, 68–80.

Bouška, V., Pešek, J., Sýkorová, I., 2000. Probable modes of occurrence of chemical elements in coal. Acta Montana. Serie B, Fuel, Carbon, Mineral Processing 10, 53–90 (Praha).

Chi, Q., Yan, M., 2007. Handbook of Elemental Abundance for Applied Geochemistry. Geological Publishing House, Beijing (in Chinese with English abstract).

Chung, F.H., 1974a. Quantitative interpretation of X-ray diffraction patterns of mixtures. I. Matrix-flushing method for quantitative multicomponent analysis. J. Appl. Crystallogr. 7, 519–525.

Chung, F.H., 1974b. Quantitative interpretation of X-ray diffraction patterns of mixtures. II. Adiabatic principle of X-ray diffraction analysis of mixtures. J. Appl. Crystallogr. 7, 526–531.

Chung, F.H., 1975. Quantitative interpretation of X-ray diffraction patterns of mixtures. III. Simultaneous determination of a set of reference intensities. J. Appl. Crystallogr. 8, 17–19.

Dai, S., Ren, D., Chou, C., Li, S., Jiang, Y., 2006. Mineralogy and geochemistry of the no. 6 coal (Pennsylvanian) in the Junger Coalfield, Ordos Basin, China. Int. J. Coal Geol. 66, 253–270.

Dai, S., Wang, X., Chen, W., Li, D., Chou, C., Zhou, Y., Zhu, C., Li, H., Zhu, X., Xing, Y., Zhang, W., Zou, J., 2010. A high-pyrite semianthracite of Late Permian age in the Songzao Coalfield, southwestern China: mineralogical and geochemical relations with underlying mafic tuffs. Int. J. Coal Geol. 83, 430–445.

Dai, S., Wang, X., Zhou, Y., Hower, J.C., Li, D., Chen, W., Zhu, X., Zou, J., 2011. Chemical and mineralogical compositions of silicic, mafic, and alkali tonsteins in the late Permian coals from the Songzao Coalfield, Chongqing, Southwest China. Chem. Geol. 282 (1–2), 29–44.

Dai, S., Zou, J., Jiang, Y., Ward, C., Wang, X., Li, T., Xue, W., Liu, S., Tian, H., Sun, X., Zhou, D., 2012a. Mineralogical and geochemical compositions of the Pennsylvanian coal in the Adaohai Mine, Daqingshan Coalfield, Inner Mongolia, China: modes of occurrence and origin of diaspore, gorceixite, and ammonian illite. Int. J. Coal Geol. 94, 250–270.

Dai, S., Ren, D., Chou, C., Finkelman, R.B., Seredin, V.V., Zhou, Y., 2012b. Geochemistry of trace elements in Chinese coals: a review of abundances, genetic types, impacts on human health, and industrial utilization. Int. J. Coal Geol. 94, 3–21.

Dai, S., Jiang, Y., Ward, C.R., Gu, L., Seredin, V.V., Liu, H., Zhou, D., Wang, X., Sun, Y., Zou, J., Ren, D., 2012c. Mineralogical and geochemical compositions of the coal in the Guanbanwusu Mine, Inner Mongolia, China: further evidence for the existence of an Al (Ga and REE) ore deposit in the Jungar Coalfield. Int. J. Coal Geol. 98, 10–40.

Dai, S., Li, T., Seredin, V.V., Ward, C.R., Hower, J.C., Zhou, Y., Zhang, M., Song, X., Song, W., Zhao, C., 2014. Origin of minerals and elements in the Late Permian coals, tonsteins, and host rocks of the Xinde Mine, Xuanwei, eastern Yunnan, China. Int. J. Coal Geol. 121, 53–78.

Dai, S., Li, T., Jiang, Y., Ward, C.R., Hower, J.C., Sun, J., Liu, J., Song, H., Wei, J., Li, Q., Xie, P., Huang, Q., 2015a. Mineralogical and geochemical compositions of the Pennsylvanian coal in the Hailiushu Mine, Daqingshan Coalfield, Inner Mongolia, China: implications of sediment-source region and acid hydrothermal solutions. Int. J. Coal Geol. 137, 92–110.

Dai, S., Seredin, V.V., Ward, C.R., Hower, J.C., Xing, Y., Zhang, W., Song, W., Wang, P., 2015b. Enrichment of U–Se–Mo–Re–V in coals preserved within marine carbonate successions: geochemical and mineralogical data from the Late Permian Guiding Coalfield, Guizhou, China. Mineral. Deposita 50, 159–186.

Dai, S., Graham, I.T., Ward, C.R., 2016. A review of anomalous rare earth elements and yttrium in coal. Int. J. Coal Geol. 159, 82–95.

Drits, V.A., Lindgreen, H., Salyn, A.L., 1997. Determination of the content and distribution of xed ammonium in illite-smectite by X-ray diffraction: application to North Sea illite-smectite. Am. Mineral. 82, 79–87.

Eskenazy, G.M., 1987. Rare earth elements and yttrium in lithotypes of Bulgarian coals. Org. Geochem. 11, 83–89.

Fu, Y., Wu, C., 2012. Study on gas-bearing characteristics of major coal seams and controlling geologic factors in Yangquan Mine Area. China Coalbed Methane 9, 21–24 (in Chinese with English abstract).

GB/T 14506.30-2010. (National Standard of P.R. China), 2011. Methods for Chemical Analysis of Silicate Rocks-Part 30: Determination of 44 Elements (in Chinese).

GB/T 15224.1-2004 (National Standard of P.R. China), 2004. Classification for Quality of Coal. Part 1: Ash Yield (in Chinese).

GB/T 15224.2-2004 (National Standard of P.R. China), 2004. Classification for Quality of Coal. Part 2: Sulfur Content (in Chinese).

GB/T 482-2008 (National Standard of P.R. China), 2008. Sampling of Coal in Seam (in Chinese).

Ge, B., Yin, G., Li, C., 1985. A preliminary study on sedimentary environments and law of coal-bearing formation in Yangquan, Shanxi. Acta Sedimentol. Sin. 3 (3), 33–44 (in Chinese with English abstract).

Goodarzi, F., Swaine, D.J., 1994a. The influence of geological factors on the concentration of boron in Australian and Canadian coals. Chem. Geol. 118, 301–318.

Goodarzi, F., Swaine, D.J., 1994b. Paleoenvironmental and environmental implications of the boron content of coals. Geol. Surv. Can. Bull. 471, 1–46.

Hayashi, K.I., Fujisawa, H., Holland, H.D., Ohmoto, H., 1997. Geochemistry of 1.9 Ga sedimentary rocks from northeastern Labrador, Canada. Geochim. Cosmochim. Acta 61, 4115–4137.

He, B., Xu, Y.-G., Zhong, Y.-T., Guan, J.P., 2010. The Guadalupian–Lopingian boundary mudstones at Chaotian (SW China) are clastic rocks rather than acidic tuffs: implication for a temporal coincidence between the end-Guadalupian mass extinction and the Emeishan volcanism. Lithos 119, 10–19.

Higashi, S., 2000. Ammonium-bearing mica and mica/smectite of several pottery stone nd pyrophyllite deposits in Japan: their mineralogical properties and utilization. Appl. Clay Sci. 16, 171–184.

Hower, J.C., Ruppert, L.F., Eble, C.F., 1999. Lanthanide, yttrium, and zirconium anomalies in the Fire Clay coal bed, Eastern Kentucky. Int. J. Coal Geol. 39, 141–153.

Jiang, Y., Zhao, L., Zhou, G., Wang, X., Zhao, L., Wei, J., Song, H., 2015. Petrological, mineralogical, and geochemical compositions of Early Jurassic coals in the Yining Coalfield, Xinjiang, China. Int. J. Coal Geol. 152, 47–67.

Jiao, X., Wang, Y., 1999. Depositional environments of the coal-bearing strata and their controls on coal seams in the Yangquan Mining District, Shanxi. Sediment. Facies Paleogeogr. 19, 30–39 (in Chinese with English abstract).

Lewińska-Preis, L., Fabiańska, M.J., Ćmiel, M., Kita, A., 2009. Geochemical distribution of trace elements in Kaffioyra and Longyearbyen coals, Spitsbergen, Norway. Int. J. Coal Geol. 80, 211–223.

Liang, S., 1996. A restudy on the tonstein composition in coal seams 3# and 12#, the third coal mine of Yangquan, Shanxi. Shanxi Min. Inst. Learned J. 14, 312–320 (in Chinese with English abstract).

Liang, S., Wang, S., Ren, D., Yao, G., 1996. Study on tobelite-bearing tonsteins of Carboniferous-Permian coal measures in North China. Coal Geol. Explor. 24, 11–18 (in Chinese with English abstract).

Lin, X., 1990. X-ray Diffraction Analytical Technology and Its Geological Application. Petroleum Industry Press, Beijing (in Chinese).

Liu, Y., Cao, L., Li, Z., Wang, H., Chu, T., Zhang, R., 1984. Elemental geochemistry. Science Press, Beijing (in Chinese).

Liu, Q., Zhang, P., Ding, S., Lin, X., Zheng, N., 1996. Ammonian illite in Permo-Carboniferous coal-bearing strata, North China. Chin. Sci. Bull. 41 (8), 717–719 (in Chinese).

Liu, Q., Zheng, L., Shen, S., Cheng, H., Liu, L., 2009. Study on the thermal stability of ammonium illite. Acta Mineral. Sin. 29, 277–282 (in Chinese with English abstract).

Liu, J., Zong, Y., Yan, X., Ji, D., Yang, Y., Hu, L., 2015. Modes of occurrence of highly-elevated trace elements in superhigh-organic-sulfur coals. Fuel 156, 190–197.

Lv, S., Shao, L., Wu, M., Jones, T., Merolla, L., Richard, R.J., 2006. Study on the correlation of bioactivity and trace elements in $PM_{10}$ from Beijing City. Sci. Sin. Terrae 36, 777–784 (in Chinese).

Permana, A.K., Ward, C.R., Li, Z., Gurba, L.W., 2013. Distribution and origin of minerals in high-rank coals of the South Walker Creek area, Bowen Basin, Australia. Int. J. Coal Geol. 116–117, 97–108.

Qin, Y., Zhang, D., Fu, X., Lin, D., Ye, J., Xu, Z., 1999. A discussion of correlation of modern tectonic stress field to physical properties of coal reservoirs in central and southern Qinshui Basin. Geogr. Rev. 45 (6), 576–583 (in Chinese with English abstract).

Rajabzadeh, M.A., Ghorbani, Z., Keshavarzi, B., 2016. Chemistry, mineralogy and distribution of selected trace-elements in the Parvadeh coals, Tabas, Iran. Fuel 174, 216–224.

Ren, D., Zhao, F., Dai, S., Zhang, J., Luo, K., 2006. Geochemistry of Trace Elements in Coal. Science Press, Beijing (556 pp). (in Chinese with English abstract).

Sahoo, P.K., Tripathy, S., Panigrahi, M.K., Equeenuddin, S.M., 2014. Geochemical characterization of coal and waste rocks from a high sulfur bearing coalfield, India: implication for acid and metal generation. J. Geochem. Explor. 145, 135–147.

Seredin, V.V., 1996. Rare earth element-bearing coals from the Russian Far East deposits. Int. J. Coal Geol. 30, 101–129.

Seredin, V.V., Dai, S., 2012. Coal deposits as a potential alternative source for lanthanides and yttrium. Int. J. Coal Geol. 94, 67–93.

Shi, S., Liu, Q., Sun, J., Wu, Z., Sun, B., 2014. Enrichment features and causes of boehmite in high-alumina partings of Junger coalfield. Coal Eng. 46, 116–122 (in Chinese with English abstract).

Sia, S., Abdullah, W.H., 2011. Concentration and association of minor and trace elements in Mukah coal from Sarawak, Malaysia, with emphasis on the potentially hazardous trace elements. Int. J. Coal Geol. 88, 179–193.

Song, X., Shao, L., Zheng, Q., Yang, S., 2014. Mineralogical and geochemical composition of particulate matter ($PM_{10}$) in coal and non-coal industrial cities of Henan Province, North China. Atmos. Res. 143, 462–472.

Song, X., Shao, L., Yang, S., Song, R., Sun, L., Cen, S., 2015a. Trace elements pollution and toxicity of airborne $PM_{10}$ in a coal industrial city. Atmos. Pollut. Res. 6, 469–475.

Song, X., Shao, L., Zheng, Q., Yang, S., 2015b. Characterization of crystalline secondary particles and elemental composition in $PM_{10}$ of North China. Environ. Earth Sci. 74, 5717–5727.

Sutcu, E.C., Karayigit, A.I., 2015. Mineral matter, major and trace element content of the Afşin-Elbistan coals, Kahramanmaraş, Turkey. Int. J. Coal Geol. 144–145, 111–129.

SY/T 5163-2010 (Petroleum and Gas Industry Standard of P.R. China), 2010. Analysis Method for Clay Minerals and Ordinary Non-clay Minerals in Sedimentary Rocks by the X-ray Diffraction (in Chinese).

Tang, Y., Cheng, A., Wang, H., Wang, S., Zhang, Z., Xie, X., Zhang, Q., Wang, C., Jia, L., 2013. Coal quality characteristic analysis of Taiyuan Formation and Shanxi Formation in Shanxi Province. Coal. Sci. Technol. 41, 10–15 (in Chinese with English abstract).

Tozsin, G., 2014. Hazardous elements in soil and coal from the Oltu coal mine district, Turkey. Int. J. Coal Geol. 131, 1–6.

Wang, Y., Qin, H., Jiao, X., 1998. Features and formation mechanism of geological structure in Yangquan Mining Area. Coal Geol. Explor. 6, 24–27 (in Chinese with English abstract).

Wang, W., Qin, Y., Liu, X., Zhao, J., Wang, J., Wu, G., Liu, J., 2011a. Distribution, occurrence and enrichment causes of gallium in coals from the Jungar Coalfield, Inner Mongolia. Sci. Sin. Terrae 41, 181–196 (in Chinese).

Wang, X., Dai, S., Ren, D., Yang, J., 2011b. Mineralogy and geochemistry of Al-hydroxide/oxyhydroxide minerals-bearing coals of the Late Paleozoic age from the Weibei coalfield in southeastern Ordos Basin, China. Appl. Geochem. 26, 1086–1096.

Ward, C.R., 2002. Analysis and significance of mineral matter in coal seams. Int. J. Coal Geol. 50, 135–168.

Ward, C.R., 2016. Analysis, origin and significance of mineral matter in coal: an updated review. Int. J. Coal Geol. 165, 1–27.

Ward, C.R., Spears, D.A., Booth, C.A., Staton, I., Gurba, L.W., 1999. Mineral matter and trace elements in coals of the Gunnedah Basin, New South Wales, Australia. Int. J. Coal Geol. 40, 281–308.

Wu, Z., Sun, J., Zhang, Z., Shi, S., Liu, Q., 2013. Discussion on feature if high alumina coal resources in Zhungeer coalfield. Coal Eng. 10, 115–118 (in Chinese with English abstract).

Xu, S., Sun, H., 2009. Analysis of resources and assurance for coal in Yangquan Mining District. J. Shanxi Coal-Min. Adm. Coll. 2, 27–28 (in Chinese).

Xu, T., Wang, X., Zhang, Y., Zhao, X., Bao, Y., 2003. Clay Minerals of Petroliferous Basins in China. Petroleum Industry Press, Beijing, pp. 535–537 (in Chinese).

Zhao, X., Zhang, Y., 1990. Clay Minerals and Clay Mineral Analysis. China Ocean Press, Beijing, pp. 21–34 (in Chinese).

Zheng, L., Liu, G., Wang, L., Chou, C.L., 2008. Composition and quality of coals in the Huaibei Coalfield, Anhui, China. J. Geochem. Explor. 97, 59–68.

Zheng, Q., Liu, Q., Shi, S., 2016. Mineralogy and geochemistry of ammonian illite in intra-seam partings in Permo-Carboniferous coal of the Qinshui Coalfield, North China. Int. J. Coal Geol. 153, 1–11.

Zhu, Y., 2013. Prospect and development of coal seam gas industry in Yangquan Mining District. Gas Technology 4, 14–17 (in Chinese).